Dynamic Synthesis of Nanodispersed C–N Crystalline Phases[1]

A.A. Sivkov, A.S. Saigash, and A.J. Pak

Tomsk Polytechnic University, 30, Lenina ave., Tomsk, 634050, Russia
Phone: +8(3822) 56-36-82, E-mail: mpt@eltil.tpu.ru

Abstract – This paper describes the results of the experiments on direct dynamic gas-phase synthesis of C–N crystalline phases, carbon nitride in particular.

The existence of crystalline covalent carbon nitride with sp^3-bonded carbon was theoretically proven about 20 years ago. However, some researchers [1, 2] say that so far there is no absolutely reliable data on the crystalline C_3N_4 synthesis. This paper describes the results of the experiments on direct dynamic gas-phase synthesis of C–N crystalline phases, carbon nitride in particular.

The composition of source components C and N and high *p*, *T* parameters necessary to form crystalline carbon nitride by a dynamic method, could be obtained in the pressure shock of the leading shock wave of a pulsed supersonic carbon electric-discharge plasma jet streaming to the camera filled with gaseous nitrogen. Such conditions can be created by a high-current (~ 150 kA) pulsed (~ 500 μs) coaxial magnetiшplasma accelerator (CMPA) with a graphite accelerating channel (AC) [4]. Source carbon in the form of nanodispersed powder (carbon) was loaded to the zone of formation of high-current *Z*-pinch discharge plasma structure accelerated in the coaxial system. The plasma was shot to an air-tight reactor chamber filled with gaseous nitrogen. About one hour after cooling and precipitation of the suspended particles the chamber was opened and the synthesized product extracted. The obtained dark-brown fine-dispersed powder was, without any preliminary treatment, analyzed by X-ray diffractometry (XRD) (Shimadzu XRD6000 (CuK_α) diffractometer), scanning-electron microscopy (SEM) (Quanta 200 3D) in combination with energy-dispersive X-ray analysis (EDAX), transmission microscopy, and phase analysis (Philips SM 30).

Analysis of close-up (× 120000) SEM micropgraphs (Fig. 1) showed that the product of the dynamic synthesis consisted mainly of spheric particles, less than 400 nm in size, and long structures, 30–40 nm in the cross section which are likely to be multilayer carbon nanotubes (MCN).

The composition and ratio of basic elements (At%) in the synthesized product were identified by the energy dispersive analysis: C – 85÷88%; N – 9÷7%; O – 6÷4%; W – 0.05÷0.1%. The method is known to overestimate carbon content. As for the oxygen, it is always present in commercially pure nitrogen (up to 10%); the nanodispersed powder also absorbed it in small amounts from the air.

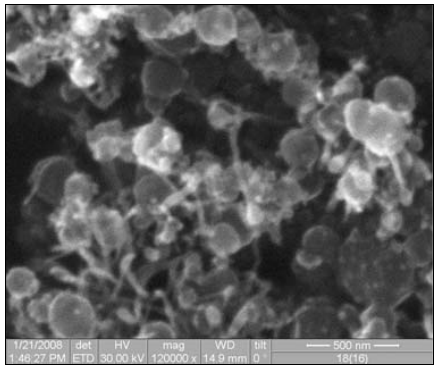

Fig. 1. SEM micrograph of the product of the C–N system direct synthesis. Zoom ×120 000

The product contained a little tungsten due to the erosion on the central electrode of the *Z*-pinch accelerator. The X-ray diffraction spectrum of the powder (Fig. 2) points at the presence of several superdispersed crystalline (and amorphous) phases there.

The full profile structural and phase analysis carried out using PowderCell 2.4 involved the study of standard spectra from the data bases as well as theoretical spectra of hypothetical carbon nitride crystalline phases [5].

The analysis showed that the majority of crystalline phases are multilayer carbon nanotubes, synthetic diamond, carbon nitride with tetragonal structure t-C_3N_4, trigonal-rhombohedral structure α-C_3N_4, and W_2C with trigonal structure. In addition, obvious presence of cubic carbon nitride c-C_3N_4 phase was observed. However, it was difficult to estimate its exact content due to subtle amounts of W_2C which has strong reflection at the same angles 2Θ.

Figure 2 and the Table show that the principal lines of the said phases in the diffraction spectrum are very close to each other, which strongly impedes the structural and phase analysis. Therefore, the ratio obtained as a result of the analysis cannot be considered reliable. In support of the hypothesis [3] about the preferential formation of pure carbon phases in the C–N system gas-phase synthesis, it was demonstrated that those phases dominate on the product content.

[1] The study was performed with financial support of the Russian Fund of Federal Property (RFFI) (Project No. 07-08-00804).

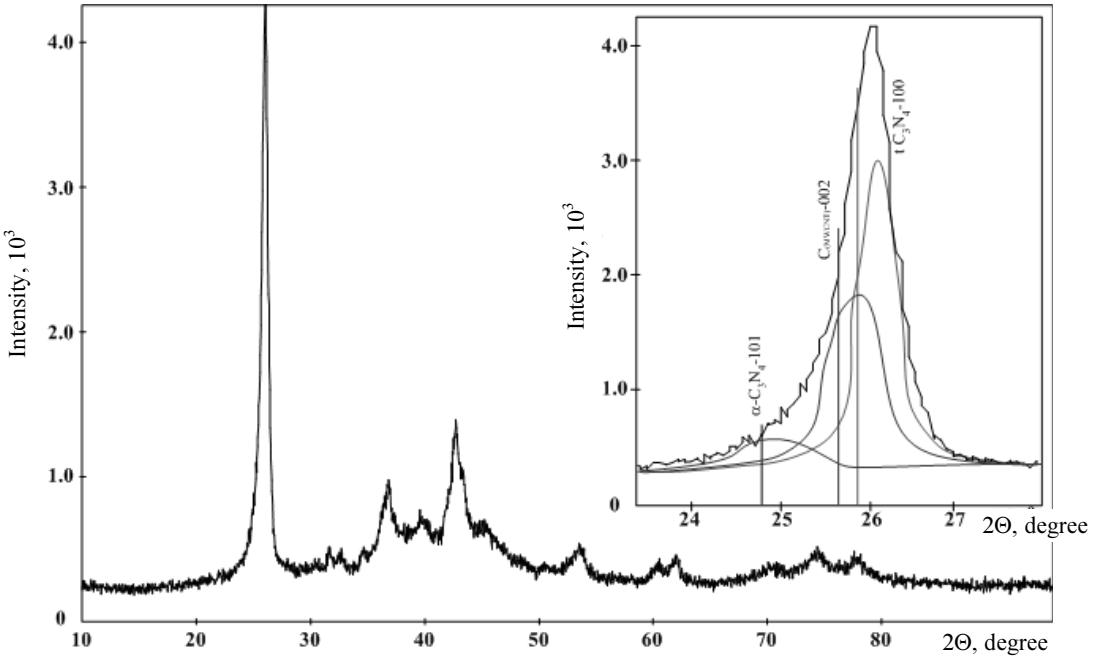

Fig. 2. X-ray diffraction pattern of the synthesized product

Table. Results of full profile analysis of X-ray diffraction spectrum

Phase	*h k l*	2Θ		Interplanar spacing *d*, Å		Content, % mass	Spacing parameters a/c		CSR, nm	$\Delta d/d \cdot 10^{-3}$
		exper.	theor.	exper.	theor.		exper.	theor.		
C (MCN)	0 0 2 1 0 1 0 0 4	25.641 44.369 52.693	25.995 44.328 53.463	3.4714 2.0400 1.7357	3.4250 2.0418 1.7125	33.73	2.4644 6.9428	2.4700 6.8500	19.07	7.76
*C*diam.	1 1 1 2 2 0 3 1 1	42.947 73.424 89.011	43.930 75.295 91.488	2.1042 1.2886 1.0989	2.0594 1.2611 1.0755	35.99	3.6446	3.5770	7.8	4.86
tC_3N_4	1 0 0 1 1 1 0 0 2	25.916 45.747 53.429	26.008 45.878 53.493	3.4352 1.9817 1.7135	3.4232 1.9764 1.7116	10.89	3.4352 3.4770	3.4232 3.4232	20.86	1.83
α-C_3N_4	1 0 1 2 0 1 1 0 2	24.767 37.227 41.940	24.679 37.332 41.569	3.5919 2.4134 2.1524	3.6045 2.4068 2.1707	19.14	6.5169 4.6567	6.4665 4.7097	10.63	6.0
cC_3N_4	2 1 1 2 2 0 3 2 1	41.353 48.122 65.279	40.559 47.184 63.936	2.1816 1.8893 1.4282	2.2224 1.9247 1.4549	–	5.3438	5.4438	11.54	6.37
W_2C	1 1 0 0 0 2 1 1 1	35.036 37.249 39.844	34.536 38.067 39.593	2.5591 2.4120 2.2607	2.5950 2.3620 2.2744	0.25	5.1182 4.8240	5.1900 4.7240	9.5	7.39

A rather striking difference between experimentally obtained values of crystallographic parameters and reference and calculated data could be explained by high microstresses, inaccurate calculated data and errors of the full profile analysis of multiphase and polymorphic system spectrum. Present dissolved oxygen has also had an impact.

Analysis of transmission electron microscopy results (Fig. 3) showed four main types of nanoobjects in the composition of the synthesized product. The objects-1 were beyond any doubt identified as multilayer carbon nanotubes using the available data (Fig. 3, *c*). Their cross section is ~ 10÷30 nm in diameter, which equals on average the coherent-scattering region (CSR) area of the C(MCN) phase (Table).

The objects-2 are relatively big, 100÷300 nm, rounded aggregates with visible natural faceting

(Fig. 3, *d*). All such objects have close-packed polycrystalline high performance and highly ordered nanostructure and resemble segments of pineapple. Several crystallites of the structure are wedge-shaped.

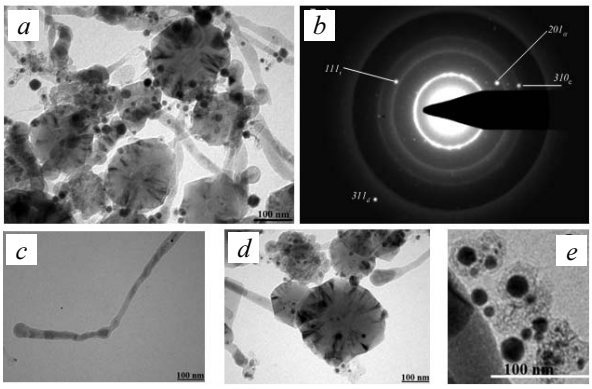

Fig. 3. General view of the product (*a*) electron-diffusion pattern of the whole area (*b*) and individual objects (*c*, *d*, *e*) whose mixture compose the synthesized product

The objects-3 are rather small, ~ 5÷25 nm, unilluminated by the electron beam (dark in the picture) spheroidal particles (Fig. 3, *e*). The biggest among them demonstrate a visible regular faceting. The majority of the particles are close to or on the surface of the big objects.

Aggregates of very small particles with an unclear morphology were defined as the objects-4.

In the electron diffraction pattern of the aggregate of nanoobjects in question (Fig. 3, *b*) there are four clearly visible continuous Debye diffraction rings. The two first rings are relatively wide due to the presence of a great number of microreflections of several nanodispersed phases. The fact that the product contains a significant number of carbon nanotubes is explained by the formation of four Debye rings. Against the background of the first ring there are very clear twinning diffraction reflections on the planes (100) t-C_3N_4 and (101) α-C_3N_4. The second ring is a superposition of microreflections of the nanotubes, nanodiamond, and t-C_3N_4. In the third ring, there is a distinct strong diffraction reflection on the plane (310) of the hypothetic cubic carbon nitride c-C_3N_4 phase crystal. In addition, there are very strong individual reflections of (111) t-C_3N_4, (201) α-C_3N_4, and (311) C (diamond) in the electron diffraction pattern.

In order to identify phases and the selected objects, we singled out a relatively small aggregate of particles with a minimum content of nanotubes (Fig. 4). This is why the diffraction pattern of this accumulation does not show the third and fourth Debye rings. In the first ring there are very distinct twinning reflections of C_3N_4 phases.

The dark-field picture of this aggregate (Fig. 4, *c*) was obtained by stopping the aperture diaphragm on one of the strongest crystalline carbon nitride reflections of the first Debye ring. Dark-field micrographs on other outstanding reflections of this ring and outside it corresponding to C_3N_4 have a similar appearance. It is obvious that the bright wedge-shaped areas are symmetrical sectors of the objects-2. They have the geometry of crystallographic planes of hypothetic crystalline phases with the cubic, pseudocubic and rhomboedric structure. The overlay of several images shows that the objects-2 are a spheroid consisting of simmetrically arranged with respect to the centre C_3N_4 crystals.

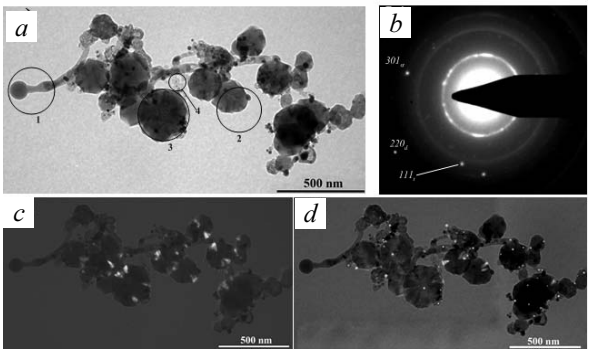

Fig. 4. Micrograph of the nanoobjects aggregate with a minimum number of nanotubes (*a*) diffraction of electrons on this aggregate (*b*), and dark-field images within the first (*c*) and second (*d*) Debye rings

The aperture diaphragm on the second ring produced dark-field image of the same aggregate (Fig. 4, *d*) with multiple bright objects-3 which are, consequently, nano-sized crystals of synthetic diamond.

Figures 5, *a* and *b* show microelectron pictures of separate objects-2 with individual objects-3 on their surface.

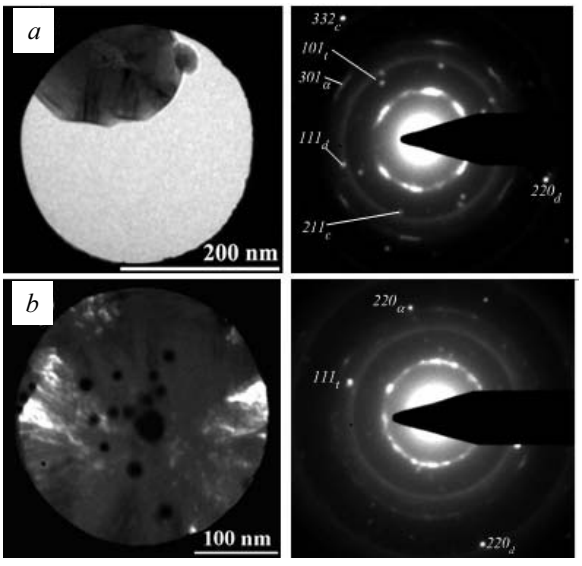

Fig. 5. Diaphragmed micropictures of the objects-2 (*a*) with the objects-3 on their surface (*b*) and corresponding electron-diffusion patterns

The areas singled out by electron beam diaphragming are circled in the micrograph of the nanoobjects accumulation (Fig. 4). It is obvious that under such conditions micro-electron diffraction patterns show

only multiple reflections of C_3N_4 crystalline phases forming a discontinuous ring, individual reflections of these phases and the synthetic diamond phases.

Figure 6 is a microelectron photograph of an area filled with small nanoparticles which is similar to the diaphragmed area 4 (Fig. 4, *a*). The corresponding electron diffraction pattern shows easily identified diffraction reflections corresponding to all crystalline phases under study.

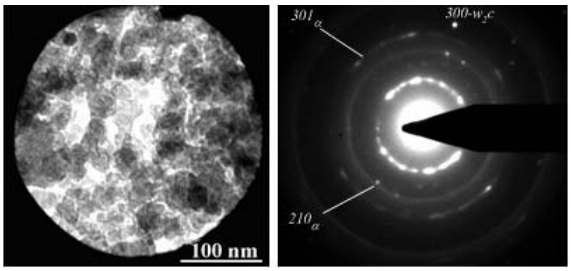

Fig. 6. Diaphragmed micropicture of the area with the accumulation of the smallest particles, and the corresponding electron-diffusion pattern

It is visible in the micropictures of aggregates of nanoobjects that the shape of the nanotubes is far from perfect. Their cross sections vary due to the distribution of various nanoparticles. The diaphragmed photograph (Fig. 7) of one of the most distinctive lengths of an individual nanotube very clearly shows the structure and geometry of nano-sized inclusions. A round inclusion at the end of the nanotube is very similar in its structure to an object-2. Other inclusions have wedge-shaped configuration. The diffraction of electrons on this object points at the presence of C_3N_4 crystalline phases with weak broadened reflections which can be seen within a strongly diffused first Debye ring.

These observations provide grounds to assume that C_3N_4 crystallites formed promote the growth of multilayer carbon nanotubes.

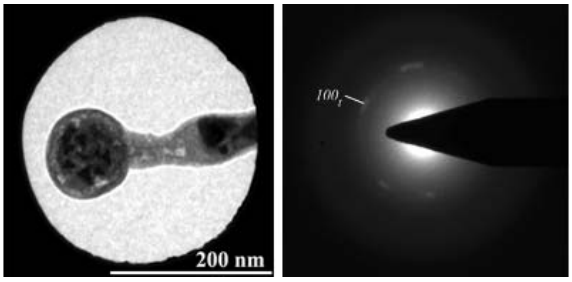

Fig. 7. Diaphragmed micropicture of a typical length of a carbon nanotube and its electron diffraction pattern (*diffraction pattern of this length*)

This experimental data is reliable enough to make a reasonably grounded supposition about the possibility of the direct synthesis of nanodispersed crystalline carbon nitride in the gaseous system of the supersonic electric-discharge carbon plasma jet streaming to the nitrogen atmosphere. The main challenge facing further research is the necessity to create conditions to significantly reduce or exclude the probability of the formation of purely carbon phases. Besides, there is a need to ensure that unnecessary materials are eliminated from the process, particularly tungsten (or any other metal) which is eroded on the central electrode of the accelerator.

References

[1] D.V. Batov and E.V. Polyakov, Hard Materials **3**, 18 (2004).

[2] B.L. Korsunsky and V.I. Pepekin, Isp. Khimii **11**/66, 1003 (1997).

[3] V.V. Odintsov and V.I. Pepekin, Dokl. Ross. Akad. Nauk. Khimiya **2**/343, 210 (1995).

[4] D.Yu. Gerasimov, A.S. Saigash, and A.A. Sivkov, *Patent RU 61856*, 2007.

[5] D.M. Teter and R.J. Hemley, Sci. **5245**, 53 (1996).